Fizika Nizkikh Temperatur, 2002, v. 28, No. 7, p. 709–715

Spin-phonon interaction and mode softening in NiF_2

D. J. Lockwood

Institute for Microstructural Sciences, National Research Council, Ottawa, ON KIA OR6
E-mail: David.Lockwood@nrc.ca

Received October 29, 2001

The temperature dependence of the four Raman-active phonons in NiF_2 has been investigated at temperatures above and below the antiferromagnetic ordering temperature of $T_N = 73$ K. All four modes exhibit distinct anomalies in their intensities and frequencies near T_N due to spin-phonon coupling. The phonon linewidths also exhibit weak anomalies. From the temperature dependences of the phonon frequencies, estimates are made of the spin-phonon coupling coefficients. The B_{1g} phonon exhibits anomalous mode softening with decreasing temperature from 300 K to T_N .

PACS: 78.30.Hv, 75.50.Ee, 63.20.Dj, 63.20.Kr

Dedicated to Professor Victor V. Eremenko on the occasion of his 70th birthday

1. Introduction

Although there have, by now, been numerous light scattering measurements of magnetic excitations in solids [1], much less is known from such studies of their interactions with phonons. This is because direct interactions of magnons, or higher lying excitons, with phonons are less likely in the range of wave vectors near the Brillouin zone center accessed in Raman spectroscopy. Nevertheless, such strong interactions have been observed, for example, in $FeCl_2 2H_2O$, $CsCoCl_3$, and $RbCoCl_3$, where there is an accidental near-degeneracy of the magnon and phonon frequencies [2]. More generally, spin-phonon interactions manifest themselves through modifications to the normal temperature dependences of the optic phonons. The exchange coupling between magnetic ions influences the phonon frequency, integrated intensity, and linewidth. Such spin-dependent effects have been reported in the phonon Raman spectra of $KCoF_3$, VI_2 , $CsCoBr_3$, EuSe, EuTe, EuO, EuS, $CdCr_2S_4$, and $CdCr_2Se_4$ [2,3]. Of the transition metal fluorides with the rutile structure, which are the main concern of this work, detailed results and comparisons with theory have been reported for the antiferromagnets FeF_2 and MnF_2 [4–8], and the diluted antiferromagnet $Fe_{1-x}Zn_xF_2$ [9]. For these compounds, the Raman-active phonon frequencies and intensities, but not the linewidths, were affected to varying extents by the antiferromagnetic ordering, and from the data spin-phonon coupling coefficients were deduced [7,8]. It is of interest to determine the magnitudes of such effects, because they can also influence the magnon Raman scattering [10].

Here we report results from a temperature dependent study of the Raman active phonons in antiferromagnetic NiF_2 (T_N = 73.2 K), which has the same rutile crystal structure of FeF_2 and MnF_2 but differs in the spin alignment. Instead of lying along the crystal *c* axis, the spins in NiF_2 lie in the *ab* plane and are tilted slightly away from the principal axes. This spin canting modifies the magnetic properties of NiF_2 and gives rise to a lower «ferromagnetic» spin wave branch as well as the usual antiferromagnetic branch found in isomorphous FeF_2 and MnF_2 [11]. These unusual magnetic properties are presumed responsible for the more pronounced spin-phonon coupling reported here for NiF_2 (spin $S = 1$) compared with that observed previously in FeF_2 (S = 2) and MnF_2 (S = 5/2). Nevertheless, the anomalous effects of the exchange coupling on the phonon Raman line parameters can

be quite subtle and were not observed in the earlier temperature dependent study by Hutchings et al. [11].

2. Experiment

The single crystal of green-coloured NiF_2 used in this study was grown from the melt at Oxford University. The optical quality crystal was x-ray oriented, cut into a cuboid of dimensions 4.0×4.2×1.1 mm, and then polished with 1 μm diamond powder. For the low temperature measurements, the sample was mounted in the helium exchange-gas space of a Thor S500 continuous flow cryostat. The sample temperature was controlled to within 0.1 K and was monitored with a gold-iron/chromel thermocouple mounted on the sample surface.

The Raman spectrum was excited with 300 mW of 514.5 nm argon laser light that had been filtered with an Anaspec S300 prism monochromator. The NiF_2 crystal is essentially transparent to 514.5 nm light and there is little laser heating at this wavelength, as was also reported in an earlier study [12]. The light scattered at 90° was dispersed with a Spex 14018 double monochromator at a resolution of 2.5 cm^{-1}, detected with a cooled RCA 31034A photomultiplier, and recorded under computer control [13]. The polarization of the scattered light was analyzed with Polaroid film, but the light was then polarization scrambled before entering the monochromator. The conventional X, Y, Z orthogonal laboratory axis system that is used to describe the scattered light polarization was chosen such that X, Y, and Z were parallel to the crystal [110], [1$\bar{1}$0], and [001] directions, respectively.

3. Phonon Raman spectrum

A factor group analysis of the rutile crystal structure (space group $P4/mnm$) predicts four Raman-active modes of A_{1g}, B_{1g}, B_{2g}, and E_g symmetry, respectively [14]. The phonon Raman spectrum of NiF_2 has been reported previously by Hutchings et al. [11] and Hwang et al. [12] and we have obtained similar results from our measurements in both $X(\bullet\,\bullet)Y$ and $Z(\bullet\,\bullet)Y$ polarizations. The mode frequencies at 295 (10) K are A_{1g} = = 407.9 (414.5) cm^{-1}, B_{1g} = 71.6 (68.7) cm^{-1}, B_{2g} = = 535.3 (541.0) cm^{-1}, and E_g = 305.6 (308.0) cm^{-1}. Note the anomalous decrease in B_{1g} mode frequency with decreasing temperature, which will be discussed later. The temperature dependences of the mode frequencies are shown in Fig. 1. All modes show an anomalous change away

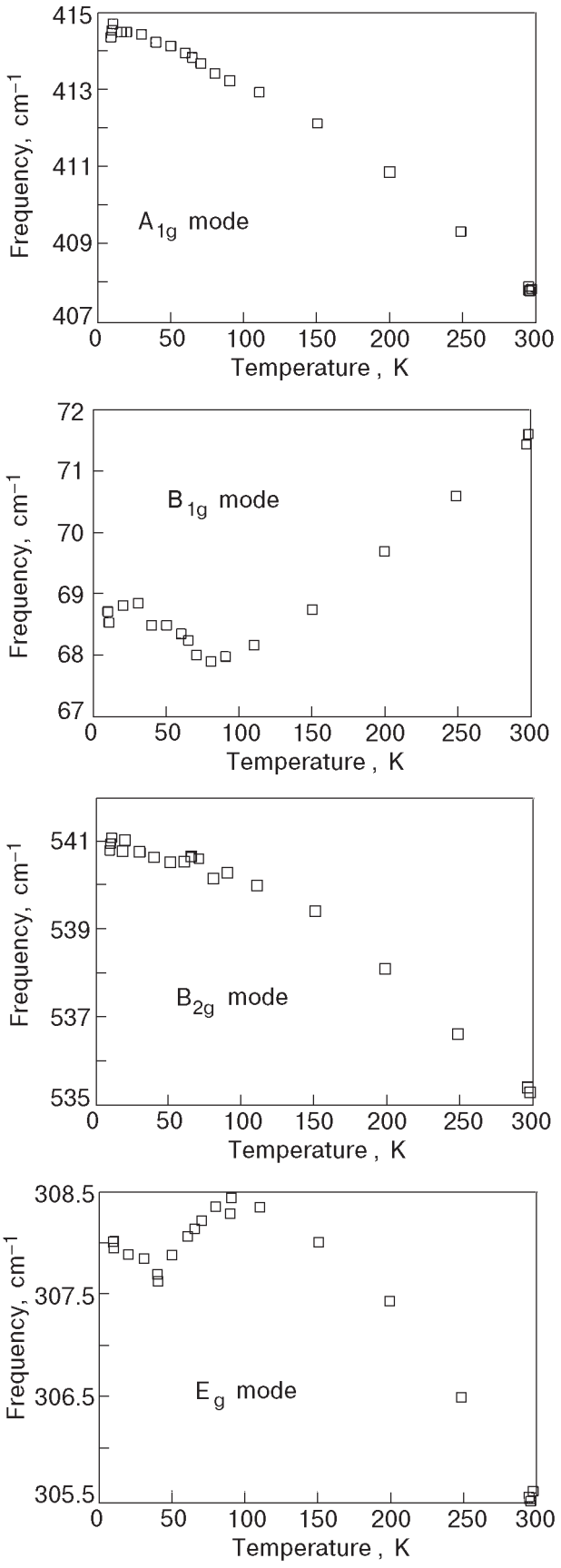

Fig. 1. Temperature dependence of the frequencies of the A_{1g}, B_{1g}, B_{2g}, and E_g Raman-active phonons in NiF_2.

from the smoothly varying behavior expected for non-magnetic rutile compounds such as MgF_2 (see Ref. 4, for example), with the A_{1g}, B_{1g}, and B_{2g} modes showing a distinct increase in frequency below T_N. In contrast, the E_g mode exhibits a decrease in frequency below T_N due to the magnetic exchange. The effect is weakest for the B_{2g} mode and strongest for the A_{1g} and B_{1g} modes.

The corresponding phonon linewidth (full width at half maximum) data are given in Fig. 2. Generally, the phonon linewidth steadily increases with increasing temperature above ~ 50 K, as is observed in other rutile compounds [4–8]. However, for the A_{1g}, B_{2g}, and E_g modes a sharp rise in the linewidth of about 20% of the 10 K value is evident at a temperature near T_N. The B_{1g} line is very sharp at all temperatures and no anomaly was detected in the linewidth at temperatures near T_N within the experimental uncertainty.

Results obtained for the temperature dependence of the integrated intensity for each mode are presented in Fig. 3. The data were all obtained in $Z(\bullet\bullet)Y$ polarization so that even though the intensity units are arbitrary the respective mode strengths are related. All modes exhibit pronounced intensity increases with decreasing temperature below ~ 100 K, being strongest for the B_{2g} mode (nearly a factor of 2 increase) and weakest for the B_{1g} mode.

4. Analysis and comparison with FeF_2 and MnF_2

In the rutile structure antiferromagnets, the exchange dependent term in the Hamiltonian may be given by [7,8]

$$H_{\text{ex}} = \sum_{i,j} J_{ij}(\mathbf{r}_1, \mathbf{r}_2, \mathbf{r}_3, \mathbf{r}_4)\mathbf{S}_i \cdot \mathbf{S}_j \qquad (1)$$

where i and j denote magnetic sites on sublattices of opposite spin orientation and J_{ij} is the dominant intersublattice exchange interaction. This exchange also depends on the position coordinates $\mathbf{r}_n$ of the four nonmagnetic F^- ions in the unit cell, because of the indirect super-exchange mechanism [15] operating in these antiferromagnets. In rutile compounds, the four Raman-active modes at the Brillouin zone center involve displacements of these F^- ions, whereas the magnetic ions remain stationary [16]. Thus these lattice vibrations all modulate J_{ij}. By using a Taylor series expansion and expressing coordinates $\mathbf{r}_n$ in terms of phonon variables, the spin-phonon coupling Hamiltonian can be derived [7,8].

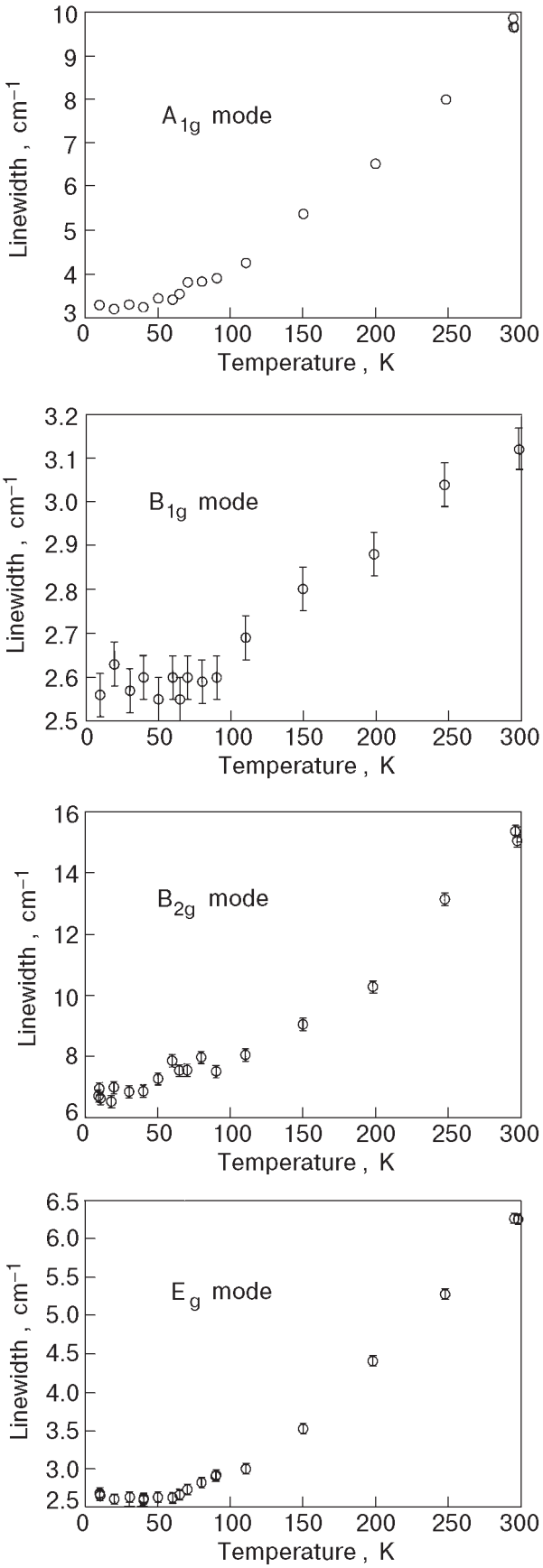

Fig. 2. Temperature dependence of the linewidths of the A_{1g}, B_{1g}, B_{2g}, and E_g Raman-active phonons in NiF_2.

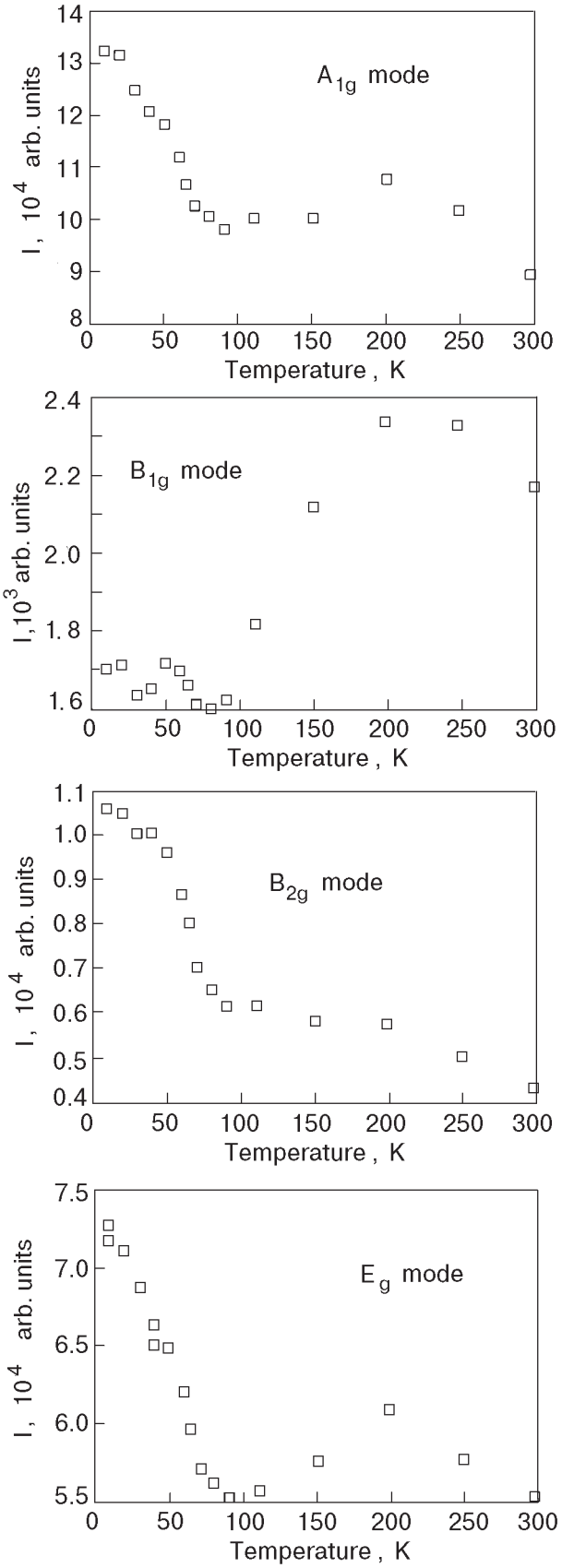

Fig. 3. Temperature dependence of the integrated intensities I of the A_{1g}, B_{1g}, B_{2g}, and E_g Raman-active phonons in NiF_2. The integration times for the A_{1g}, B_{1g}, B_{2g}, and E_g mode measurements were 1, 8, 4, and 1s, respectively.

Phonon frequencies

The result thus obtained for the renormalization of the phonon frequency ω_{ph} is [7,8]

$$\omega_{ph} = \omega_{ph}^0 + \lambda < \mathbf{S}_i \cdot \mathbf{S}_j > \qquad (2)$$

Where ω_{ph}^0 is the phonon frequency in the absence of spin-phonon coupling and $< \mathbf{S}_i \cdot \mathbf{S}_j >$ denotes a statistical mechanical average for adjacent spins on opposite sublattices. The coupling coefficient λ is different for each phonon and may have either sign. The frequency shift of the phonon due to spin dependent effects is thus

$$\Delta\omega_{ph}(T) = -\lambda < \mathbf{S}_i \cdot \mathbf{S}_j >, \qquad (3)$$

which may be rewritten as

$$\Delta\omega_{ph}(T) = -\lambda S^2 \phi(T). \qquad (4)$$

Here $\phi(T)$ is the short range order parameter defined by

$$\phi(T) = \left| < \mathbf{S}_i \cdot \mathbf{S}_j > \right| / S^2. \qquad (5)$$

For a detailed comparison of theory and experiment it is thus necessary to evaluate $\phi(T)$ at temperatures above and below T_N. Although this has not yet been done for the $S = 1$ case of NiF_2, $\phi(T)$ has been calculated for the case of $S = 2$ (FeF_2) and $S = 5/2$ (MnF_2) for temperatures up to $2T_N$. The $\phi(T)$ curves for $S = 2$ and $5/2$ are very similar over the temperature range $0 \le T \le 2T_N$ [8]. Although slight differences can be expected for the $S = 1$ case, the use of the $S = 2$ results for $\phi(T)$ should provide reasonable first estimates of the spin-phonon coupling coefficients in NiF_2. Using the $S = 2$ values for $\phi(0)$ and $\phi(2T_N)$ and by estimating $\Delta\omega_{ph}(0)$ and $\Delta\omega_{ph}(2T_N)$ from the frequency versus temperature results given in Fig. 1 in the same way as was done before [7,8] for FeF_2 and MnF_2, approximate values for λ were obtained.

Table 1

Spin-phonon coupling coefficients λ (cm^{-1}) in rutile structure antiferromagnets.

Phonon	FeF_2	MnF_2[a]	NiF_2
A_{1g}	1.3[a]/1.49[b]	−0.4	−1.6
B_{1g}	−0.4[a]	−0.3	−2.9
B_{2g}	−0.3[a]	−0.3	−0.8
E_g	0.5[a]/0.54[b]	0.2	0.9

Comment: [a] From Ref. 8, [b] From Ref. 9.

The results obtained for λ in NiF_2 are compared with the FeF_2 and MnF_2 cases in Table 1. Overall the spin-phonon coupling coefficient for each phonon is larger for NiF_2 than in FeF_2 and MnF_2 and the enhancement for the B_{1g} mode is particularly pronounced (by an order of magnitude). This may be a consequence of the low frequency of this mode in conjunction with the two spin wave branches in NiF_2. The sign of the coupling coefficients for NiF_2 and MnF_2 is the same for each phonon, and also for FeF_2 with the exception of the A_{1g} mode.

Phonon linewidths

The linewidth anomalies noted above have not been seen in MnF_2 and FeF_2 [7,8]. Phonon linewidths in crystalline solids arise from three- (and four-) phonon anharmonic interactions, with zone center modes decaying into pairs of phonons with equal and opposite wave vectors. Usually, the higher the phonon frequency the wider the Raman line, as observed here for NiF_2 (see Fig. 2), owing to the higher number of available decay paths. The low frequency B_{1g} mode can only decay into acoustic modes and hence its extreme sharpness even at room temperature. In antiferromagnets below T_N, there is an additional decay channel possible into pairs of magnons of equal and opposite wave vector. Also, as discussed in detail by Wakamura for ferrimagnetic $FeCr_2S_4$ [17], a rapid variation in optical phonon damping near T_N can be induced from the interaction between the spin ordering and phonons at or near the Brillouin zone boundary. However, the lack of an observable anomaly near T_N in MnF_2 and FeF_2 indicates that these additional decay mechanisms are not favoured for the four optic modes. However, in NiF_2 there exists the low frequency «ferromagnetic» branch, which approximates an acoustic phonon type dispersion for wave vectors away from the Brillouin zone center. It is thus feasible that phonon decays into this branch are responsible for the observed changes in linewidth of the A_{1g}, B_{2g}, and E_g modes in NiF_2 near T_N. On the other hand, the B_{1g} mode is too low in energy to avail itself of this extra decay path and thus exhibits no observable anomaly.

Phonon intensities

An expression for the phonon Raman intensities can be obtained in a similar way to that of the phonon frequencies by expanding the Raman polarizability tensor in terms of spin operators and the F^- ion displacements. The Stokes integrated intensity can be written as [7]

$$I = (n_{\text{ph}} + 1)[\left|A + B < \mathbf{S}_i \cdot \mathbf{S}_j >\right|^2 + C^2 < S^Z >^2], \quad (6)$$

where n_{ph} is the Bose population factor for phonons, and A, B, and C are constants. Coefficient A represents the intensity behavior in the absence of spin-phonon coupling.

It is not possible at this stage to separate out the two spin-dependent contributions to the Raman intensity, as the relative weights of B and C are not known. However, by using Eq. (5) and taking the mean field approximation where $\phi(T) = (< S^Z > / S)^2$, Eq. (6) can be approximated by

$$I = (n_{\text{ph}} + 1)[\left|A + BS^2\phi(T)\right|^2 + C^2S^2\phi(T)]. \quad (7)$$

At $T = 0$, $\phi(T) = 1$ and for $S = 1$ Eq. (7) becomes

$$I = (n_{\text{ph}} + 1)[\left|A + B\right|^2 + C^2]. \quad (8)$$

The integrated intensity data for the four phonons given in Fig. 3 all exhibit an increase with decreasing temperature below T_N, and reach a saturation value at $T = 0$ for the B_{1g} mode and maxima for the other modes. This indicates that the net contribution of coefficients B and C in Eq. (8) must be positive. These coefficients can, in principle, have either sign. To have some indication of the magnitude of these coefficients, we consider the case of the A_{1g} phonon. From Fig. 3 we estimate at $T = 0$ that $A^2 \simeq 9$ and that $\left|A + B\right|^2 + C^2 \simeq 13.5$ (ignoring the 10^4 multiplicative factor and the Bose factor). Thus $A \simeq 3$, and $B \simeq -3 \pm \sqrt{13.5 - C^2}$. Taking the extreme case of $B = 0$, then $|C| \simeq 2$. At the other extreme of $C = 0$, then $B \simeq 0.7$ or -7. For C to be a real quantity, we see that B cannot be less than about -7 or greater than about 0.7. Likewise for B to be real, $|C|$ cannot be greater than about 2. Thus although B and C cannot be uniquely determined at present, their magnitudes can be of the same order as A.

In the other rutile antiferromagnets FeF_2 and MnF_2, the A_{1g} and E_g modes exhibit the same marked increase in intensity with decreasing temperature below T_N as in NiF_2 [5,7]. The intensities of the B_{1g} and B_{2g} phonons in MnF_2 are not as sensitive to the magnetic ordering [7], whereas the B_{1g} phonon in FeF_2 exhibits a pronounced decrease in intensity [5]. Clearly there is a variation in the magnitudes and signs of B and C for the various phonons in the different rutile structure antiferromagnets.

5. B_{1g} mode softening

The anomalous behavior of the B_{1g} mode frequency ω_{B1g} with temperature (see Fig. 1) or pressure in rutile structure compounds such as TiO_2, SnO_2, MnF_2, and FeF_2 has been noted previously [5,6,18]. It was postulated earlier that the B_{1g} mode softening might be the precursor of a structural phase transition [19] with $\omega^2_{B1g} \propto (T - T_C)$, where T_C is the phase transition temperature. Indeed the frequency data for the B_{1g} mode in NiF_2 are an excellent fit to such a law for $T > 100$ K:

$$\omega^2_{B_{1g}} \ [\mathrm{cm}^{-2}] = \alpha T + \omega_0^2 \qquad (9)$$

with $\alpha = 2.56$ and $\omega_0^2 = 4353$. Extrapolation of ω^2_{B1g} to zero results in a virtual transition temperature T_V of −1700 K. A comparison of these NiF_2 results with those obtained earlier for FeF_2 and MnF_2 is given in Table 2 [5,6]. This Table shows that the results obtained for NiF_2 and FeF_2 are remarkably similar and not too different from those of MnF_2. Parameter T_V is a large negative number in all cases, and thus it is unlikely that such a mode softening could ever result in a structural phase transition, even if it were highly first-order in nature.

Table 2

Parameters ω_0 and α from Eq. (9) for the B_{1g} mode softening in rutile structure compounds and the virtual transition temperature T_V.

Compound	ω_0, cm^{-1}	α, $\mathrm{cm}^{-2}/\mathrm{K}$	T_V, K
MnF_2 [a]	54.2	2.37	−1240
FeF_2 [b]	67.6	2.56	−1780
NiF_2	66.0	2.56	−1700

Comment: [a] From Ref. 6, [b] From Ref. 5.

More recently, Merle et al. [20] have demonstrated that the pressure dependent softening of the B_{1g} phonon in TiO_2 does not exhibit a special sensitivity to an orthorhombic distortion and that it arises from atomic displacements associated with pure rotations of anions around the central cation. Similarly, a detailed analysis of the temperature dependent softening of the B_{1g} phonon in FeF_2 led to the conclusion that it results from the lattice thermal contraction, which disproportionally influences the forces between nearest-neighbor fluorine ions in adjacent planes perpendicular to the c axis [5]. Although a structural transition mechanism cannot strictly be ruled out, it is thus most likely that the B_{1g} phonon softening in NiF_2, which is so similar to that in FeF_2, is also a consequence of changes in the anion force constants with lattice contraction. Unfortunately, lattice dynamical models [16] for rutile structure antiferromagnets are not reliable enough to test this proposition [5]. However, further support for this viewpoint comes from a recent thorough analysis of the B_{1g} phonon temperature and pressure dependence in isostructural MgF_2. This study has confirmed that the anomalous mode softening observed with decreasing temperature in this compound is indeed caused by the thermal contraction of the lattice [21].

Conclusions

From a study of the temperature dependences of the four Raman-active modes in NiF_2, considerable spin-phonon coupling has been revealed from the phonon line parameters of frequency, linewidth, and intensity. Coupling parameters have been deduced from the phonon frequencies and were found to be larger than those for the isostructural antiferromagnets FeF_2 and MnF_2. Large intensity coupling parameters were also deduced. The anomalous softening of the B_{1g} mode with decreasing temperature is ascribed to lattice thermal contraction rather than evidence for some (virtual) structural phase transition.

Acknowledgment

The expert technical assistance of H. J. Labbe in the Raman measurements is gratefully acknoweledged.

1. M. G. Cottam and D. J. Lockwood, *Light Scattering in Magnetic Solids,* Wiley, New York, (1986).
2. For a review of this work and further references see Ref. 1, pp. 220–221.
3. For details of the spin-phonon coupling in the europium and cadmium-chromium compounds, see the extensive review by G. Guntherodt and R. Zeyher, in: *Light Scattering in Solids IV*, M. Cardona and G. Guntherodt (eds.) Springer-Verlag Heidelberg, (1984).
4. J. L. Sauvajol, R. Almairac, C. Benoit, and A. M. Bon, in: *Lattice Dynamics*, M. Balkanski (ed.) Flammarion, Paris, (1978), p. 199.
5. D. J. Lockwood, R. S. Katiyar, and V. C. Y. So, *Phys. Rev.* **B28**, 1983 (1983).
6. D. J. Lockwood, in: *Proc. IXth Intern. Conference on Raman Spectroscopy*, M. Tsuboi (ed.) *Chem. Soc. Jpn.*, Tokyo, (1984), p. 810.

7. D. J. Lockwood and M. G. Cottam, in: *Magnetic Excitations and Fluctuations II*, U. Balucani, S. W. Lovesey, M.G. Rasetti, and V. Tognetti (eds.) Springer, Berlin, (1987), p. 186.
8. D. J. Lockwood and M.G. Cottam, *J. Appl. Phys.* **64**, 5876 (1988).
9. C. Binek and W. Kleeman, *J. Phys.: Condensed Matter* **4**, 65 (1992).
10. M. G. Cottam, *J. Phys.* **C7**, 2901 (1974).
11. M. T. Hutchings, M. F. Thorpe, R. J. Birgeneau, P. A. Fleury, and H. J. Guggenheim, *Phys. Rev.* **B2**, 1362 (1970).
12. D.-M. Hwang, T. T. Chen, and H. Chang, *Solid State Commun.* **18**, 1101 (1976).
13. N. L. Rowell, D. J. Lockwood, and P. Grant, *J. Raman Spectrosc.* **10**, 119 (1981); D. J. Lockwood and C. P. Cantin, in: *Proc. XIth Intern. Conf. on Raman Spectroscopy*, R. J. H. Clark and D. A. Long (eds.) Wiley, Chichester, (1988), p. 947.
14. W. Hayes and R. Loudon, *Scattering of Light by Crystals Wiley*, New York, (1978), p. 119.
15. M. G. Cottam and D. J. Lockwood, *Light Scattering in Magnetic Solids,* Wiley, New York, (1986), p. 6.
16. R. S. Katiyar, *J. Phys.* **C3**, 1087 (1970); *ibid*. **3**, 1693 (1970).
17. K. Wakamura, *Solid State Commun.* **71**, 1033 (1989).
18. References to the pressure dependent studies of TiO_2 and SnO_2 are given in Ref. 5.
19. G. A. Samara and P. S. Peercy, *Phys. Rev.* **B7**, 1131 (1973).
20. P. Merle, J. Pascual, J. Camassel, and H. Mathieu, *Phys. Rev.* **B21**, 1617 (1980).
21. A. Perakis, E. Sarantopoulou, Y. S. Raptis, and C. Raptis, *Phys. Rev.* **B59**, 775 (1999).